

## Article

# The Higgs Trilinear Coupling and the Scale of New Physics for the SM-Axion-Seesaw-Higgs portal inflation (SMASH) Model

C.R. Das <sup>1,\*</sup> , Katri Huitu <sup>2</sup>  and Timo J. Kärkkäinen <sup>3</sup> 

<sup>1</sup> Bogoliubov Laboratory of Theoretical Physics, Joint Institute for Nuclear Research - International Intergovernmental Organization, Joliot-Curie 6, 141980 Dubna, Moscow region, Russian Federation; das@theor.jinr.ru

<sup>2</sup> Department of Physics and Helsinki Institute of Physics, P. O. Box 64, FI-00014 University of Helsinki, Finland; katri.huitu@helsinki.fi

<sup>3</sup> Institute for Theoretical Physics, ELTE Eötvös Loránd University, Pázmány Peter sétány 1/A, 1117 Budapest, Hungary; timo.karkkainen@ttk.elte.hu

\* Correspondence: das@theor.jinr.ru; Tel.: +7-962-915-9146

**Abstract:** In the extended scalar sector of the SMASH (Standard Model - Axion - Seesaw - Higgs portal inflation) framework, we conduct a phenomenological investigation of the observable effects. In a suitable region of the SMASH scalar parameter spaces, we resolve the vacuum metastability issue and discuss the one-loop correction to the triple Higgs coupling  $\lambda_{HHH}$ . The  $\lambda_{HHH}$  and SM Higgs quartic coupling  $\lambda_H$  corrections are found to be proportional to the threshold correction. A large  $\lambda_{HHH}$  correction ( $\gtrsim 5\%$ ) implies vacuum instability in the model and thus limits the general class of theories that use threshold correction. We perform a full two-loop renormalization group analysis of the SMASH model.

**Keywords:** Higgs portal inflation; Beyond the Standard Model; SMASH; Higgs triple coupling; Higgs trilinear coupling

**PACS:** 12.60.-i, 14.80.Cp, 12.10.Kt, 11.10.Hi

## 1. Introduction

After the discovery of the Standard Model (SM) Higgs boson [1,2], every elementary particle of the SM has been confirmed to exist. Even though the past forty years have been a spectacular triumph for the SM, the mass of the Higgs boson ( $m_H = 125.09 \pm 0.32$  GeV) poses a serious problem for the SM. It is well-known that the SM Higgs potential is metastable [3], as the sign of the quartic coupling,  $\lambda_H$ , turns negative at instability scale  $\Lambda_{IS} \sim 10^{11}$  GeV. On the other hand, the SM is devoid of nonperturbativity problems since the nonperturbativity scale  $\Lambda_{NS} \gg M_{Pl}$ , where  $M_{Pl} = 1.22 \times 10^{19}$  GeV is the Planck scale. In the post-Planckian regime, effects of quantum gravity are expected to dominate, and the nonperturbativity scale is therefore well beyond the validity region of the SM, unlike the instability scale. The largest uncertainties in SM vacuum stability are driven by top quark pole mass and the mass of the SM Higgs boson. The current data is in significant tension with the stability hypothesis, making it more likely that the universe is in a false vacuum state. The expected lifetime of vacuum decay to a true vacuum is extraordinarily long, and it is unlikely to affect the evolution of the universe. However, it is unclear why the vacuum state entered into a false vacuum to begin with during the early universe. In this post-SM era, the emergence of vacuum stability problems (among many others) forces the particle theorists to expand the SM in such a way that the  $\lambda_H$  will stay positive during the running all the way up to the Planck scale.

It is possible that at or below the instability scale, heavy degrees of freedom originating from a theory beyond the SM start to alter the running of the SM parameters of renormalization group equations (RGE). It has been shown that incorporating Type-I

seesaw mechanism [4–14] will have a large destabilizing effect if the neutrino Yukawa couplings are large [15], and an insignificantly small effect if they are small. Thus, to solve the vacuum stability problem simultaneously with neutrino mass, a larger theory extension is required. Embedding the invisible axion model [16–18] together with Type-I seesaw was considered in [19,20]. The axion appears as a phase of a complex singlet scalar field. This approach aims to solve the vacuum stability problem by proving that the universe is currently in a true vacuum. The scalar sector of such a theory may stabilise the vacuum with a threshold mechanism [21,22]. The effective SM Higgs coupling gains a positive correction  $\delta \equiv \lambda_{H\sigma}^2 / \lambda_\sigma$  at  $m_\sigma$ , where  $\lambda_{H\sigma}$  is the Higgs doublet-singlet portal coupling and  $\lambda_\sigma$  is the quartic coupling of the new scalar.

Corrections altering  $\lambda_H$  would in such a model also induce corrections to triple Higgs coupling,  $\lambda_{HHH}^{\text{tree}} = 3m_H^2/v$ , where  $v = 246.22 \text{ GeV}$  is the SM Higgs vacuum expectation value (VEV). The triple Higgs coupling is uniquely determined by the SM but unmeasured. In fact, the Run 2 data from the Large Hadron Collider (LHC) has only been able to determine the upper limit of the coupling to be 15 times the SM prediction [23]. Therefore, future prospects of measuring a deviation of triple Higgs coupling by the high-luminosity upgrade of the LHC (HL-LHC) [24] or by a planned next-generation Future Circular Collider (FCC) [25–27] give us hints of the structure of the scalar sector of a beyond-the-SM theory. Previous work has shown that large corrections to triple Higgs coupling might originate from a theory with one extra Dirac neutrino [28], inverse seesaw model [29], two Higgs doublet model [30–32], one extra scalar singlet [33–35] or in the Type II seesaw model [36].

The complex singlet scalar, and consequently the corresponding threshold mechanism, is embedded in a recent SMASH [37–39] theory, which utilizes it at  $\lambda_{H\sigma} \sim -10^{-6}$  and  $\lambda_\sigma \sim 10^{-10}$ . The mechanism turns out to be dominant unless the new Yukawa couplings of SMASH are  $\mathcal{O}(1)$ . In addition to its simple scalar sector extension, SMASH includes electroweak singlet quarks  $Q$  and  $\bar{Q}$  and three heavy right-handed Majorana neutrinos  $N_1$ ,  $N_2$  and  $N_3$  to generate masses for neutrinos.

The structure of this paper is as follows. In Sec. 2, we summarize the SMASH model and cover the relevant details of its scalar sector. We also establish the connection between the threshold correction and the leading order  $\lambda_{HHH}$  correction. In Sec. 3, we discuss the methods, numerical details, RGE running, and our choice of benchmark points. Our results are presented in Sec. 4, where the viable parameter space is constrained by various current experimental limits. In SMASH, one can obtain at most  $\sim 5\%$  correction to  $\lambda_{HHH}$  while simultaneously stabilizing the vacuum. We give our short conclusions on Sec. 5.

## 2. Theory

The SMASH framework [37–39] expands the scalar sector of the SM by introducing a complex singlet field

$$\sigma = \frac{1}{\sqrt{2}}(v_\sigma + \rho)e^{iA/v_\sigma}, \quad (1)$$

where  $\rho$  and  $A$  (the axion) are real scalar fields, and  $v_\sigma \gg v$  is the VEV of the complex singlet. The scalar potential of SMASH is then

$$\begin{aligned} V(H, \sigma) = & \lambda_H \left( H^\dagger H - \frac{v^2}{2} \right)^2 + \lambda_\sigma \left( |\sigma|^2 - \frac{v_\sigma^2}{2} \right)^2 \\ & + 2\lambda_{H\sigma} \left( H^\dagger H - \frac{v^2}{2} \right) \left( |\sigma|^2 - \frac{v_\sigma^2}{2} \right). \end{aligned} \quad (2)$$

In basis  $(H, \sigma)$ , the scalar mass matrix of this potential is

$$M_{\text{scalar}} = \begin{pmatrix} 2\lambda_H v^2 & 2\lambda_{H\sigma} v v_\sigma \\ 2\lambda_{H\sigma} v v_\sigma & 2\lambda_\sigma v_\sigma^2 \end{pmatrix}, \quad (3)$$

which has eigenvalues

$$m_H^2 = v^2 \lambda_H + v_\sigma^2 \lambda_\sigma - \sqrt{v^4 \lambda_H^2 + 4v^2 v_\sigma^2 \lambda_{H\sigma}^2 - 2v^2 v_\sigma^2 \lambda_H \lambda_\sigma + v_\sigma^4 \lambda_\sigma^2}, \quad (4)$$

$$m_\sigma^2 = v^2 \lambda_H + v_\sigma^2 \lambda_\sigma + \sqrt{v^4 \lambda_H^2 + 4v^2 v_\sigma^2 \lambda_{H\sigma}^2 - 2v^2 v_\sigma^2 \lambda_H \lambda_\sigma + v_\sigma^4 \lambda_\sigma^2}. \quad (5)$$

At the heavy singlet limit  $\lambda_\sigma v_\sigma^2 \gg \lambda_H v^2$

$$m_H^2 = 2v^2 \left( \lambda_H - \frac{\lambda_{H\sigma}^2}{\lambda_\sigma} \right) + \mathcal{O}\left(\frac{v^2}{v_\sigma^2}\right), \quad (6)$$

$$m_\sigma^2 = 2v_\sigma^2 \lambda_\sigma - 2v^2 \frac{\lambda_{H\sigma}^2}{\lambda_\sigma} + \mathcal{O}\left(\frac{v^4}{v_\sigma^2}\right). \quad (7)$$

Defining threshold correction  $\delta \equiv \lambda_{H\sigma}^2 / \lambda_\sigma$ ,

$$m_H^2 \approx 2v^2(\lambda_H - \delta) \equiv 2v^2 \lambda_H^{\text{SM}}, \quad m_\sigma^2 \approx 2v_\sigma^2 \lambda_\sigma - 2v^2 \delta. \quad (8)$$

The SMASH framework also includes a new quark-like field  $Q$ , which has colour but is an electroweak singlet. It gains its mass via the Higgs mechanism, through a complex singlet  $\sigma$ . It arises from the Yukawa term:

$$\mathcal{L}_Q^Y = Y_Q \bar{Q} \sigma Q \Rightarrow m_Q \approx \frac{Y_Q v_\sigma}{\sqrt{2}}. \quad (9)$$

We will show later that  $Y_Q = \mathcal{O}(1)$  is forbidden by vacuum stability requirement. The hypercharge of  $Q$  is chosen to be  $q = -1/3$ , even though  $q = 2/3$  is possible. Our analysis is almost independent of the hypercharge assignment.

**Threshold correction:** Consider an energy scale below  $m_\sigma < \Lambda_{\text{IS}}$ , where the heavy scalar  $\sigma$  is integrated out. The low-energy Higgs potential should match the SM Higgs potential:

$$V(H) = \lambda_H^{\text{SM}} \left( H^\dagger H - \frac{v^2}{2} \right)^2. \quad (10)$$

It turns out that the quartic coupling we measure has an additional term:

$$\lambda_H^{\text{SM}} = \lambda_H - \frac{\lambda_{H\sigma}^2}{\lambda_\sigma}. \quad (11)$$

Since the SM Higgs quartic coupling will be approximately  $\lambda_H(M_{Pl}) \approx -0.02$ , the threshold correction

$$\delta \equiv \frac{\lambda_{H\sigma}^2}{\lambda_\sigma} \quad (12)$$

should have a minimum value close to  $|\lambda_H(M_{Pl})|$  or slightly larger to push the high-energy counterpart  $\lambda_H$  to positive value all the way up to  $M_{Pl}$ . A too large correction will however increase  $\lambda_H$  too rapidly, exceeding the perturbativity limit  $\sqrt{4\pi}$ . We demonstrate the conditions for  $\delta$  in Sec. 4. Similar to  $\lambda_H$ , the SM Higgs quadratic parameter  $\mu_H$  gains a threshold correction:

$$\left( \mu_H^{\text{SM}} \right)^2 = \mu_H^2 - \frac{\lambda_{H\sigma}}{\lambda_\sigma} \mu_\sigma^2. \quad (13)$$

In the literature [21,22], there are two possible ways of implementing this threshold mechanism. One may start by solving the SM RGE's up to  $m_\sigma$ , where the new singlet effects kick in, and the quadratic and quartic couplings gain sudden increments. Continuation of RGE analysis to even higher scales then requires utilizing the new RGE's up to the Planck scale.

Another way is to solve the new RGE's on the SM scale, not bothering to solve the low-energy SM RGE's at all. We will use the former approach.

**One-loop correction to triple Higgs coupling:** The portal term of the Higgs potential contains the trilinear couplings for  $HH\rho$  and  $H\rho\rho$  vertices. The vertex factors for  $HH\rho$  and  $H\rho\rho$  vertices are introduced in Fig. 1. The one-loop diagrams contributing to SM triple Higgs coupling are in Fig. 2. We denote the SM tree-level triple Higgs coupling as  $\lambda_{HHH}$ . The correction is gained by adding all the triangle diagrams (taking into account the symmetry factors):

$$\begin{aligned}\Delta\lambda_{HHH} = & 3 \cdot \lambda_{HHH} \lambda_{H\sigma}^2 v_\sigma^2 I(m_H, m_H, m_\rho; p, q) \\ & + 3 \cdot \lambda_{H\sigma}^3 v v_\sigma^2 I(m_H, m_\rho, m_\rho; p, q) \\ & + 1 \cdot \lambda_{H\sigma}^3 v^3 I(m_\rho, m_\rho, m_\rho; p, q).\end{aligned}\quad (14)$$

Here  $p$  and  $q$  are the external momenta and the loop integral is defined as

$$I(m_A, m_B, m_C; p, q) = \int \frac{d^4 k}{(2\pi)^4} \frac{1}{(k^2 - m_A^2)((k-p)^2 - m_B^2)((k+q)^2 - m_C^2)}. \quad (15)$$

The process  $H \rightarrow HH$  is disallowed for on-shell external momenta, so at least one of them must be off-shell. There should be 3 contributions, corresponding to the leftmost diagram in Fig. 2, in which the out-of-shell momentum enters at different vertices. The same is true for the middle diagram, while the last diagram in the row is completely symmetrical and only one contribution should be taken into account. This logic will result in (3,3,1) symmetry coefficients for the diagrams (leftmost, middle, rightmost) in Eq. 14, if we neglect all external momenta (or consider the amplitude at symmetric point). The first diagram is dominant due to the heaviness of the  $\rho$  scalar. Therefore, we may ignore the subleading contributions of diagrams involving two or more  $\rho$  propagators. We integrate out the heavy scalar, causing the finite integral in Eq. 15 to be logarithmically divergent. We calculate the finite part of it using dimensional regularization and obtain

$$\Delta\lambda_{HHH} = -\lambda_{HHH} \frac{3\delta}{16\pi^2} \left( 2 + \ln \frac{\mu^2}{m_H^2} - z \ln \frac{z+1}{z-1} \right), \quad (16)$$

where  $z \equiv \sqrt{1 + (4m_H^2/q^2)}$  and  $\mu = m_\sigma$  is the regularization scale. We have used the modified minimal subtraction scheme ( $\overline{\text{MS}}$ ), where the terms  $\ln 4\pi$  and Euler-Mascheroni constant  $\gamma_E \approx 0.57722$  emerging in the calculation are absorbed to the regularization scale  $\mu$ . Note that the correction is dependent on the Higgs off-shell momentum  $q \equiv q^*$ , which we assume to be at  $\mathcal{O}(1)$  TeV at the LHC and HL-LHC. For calculations, we use the value  $q^* = 1$  TeV. It is especially interesting to see that at the leading order, the triple Higgs coupling correction is proportional to the threshold corrections. This intimate connection forbids a too large correction. In fact, the bound from vacuum stability turns out to constrain the triple Higgs coupling correction to  $\lesssim 5\%$ , as we shall see in Section 4. Consequently, if LHC or HL-LHC manages to measure a correction to  $\lambda_{HHH}$ , this will rule out theories that utilize exclusively threshold correction mechanisms as a viable solution to vacuum stability problem. Indeed, there are alternate ways to produce large  $\Delta\lambda_{HHH}$  without expanding the scalar sector [28,29].

It should be noted that loop corrections contributing to the final to-be-observed value are included in the SM. Indeed, experiments are measuring  $\lambda_{HHH}^{\text{SM}} = \lambda_{HHH}^{\text{SM(tree)}} + \lambda_{HHH}^{\text{SM(1-loop)}}(q^*) + \dots$ , where the SM one-loop correction depends on the Higgs off-shell momentum. At the  $\mathcal{O}(1)$  TeV scale we are considering, the SM 1-loop correction amounts to approximately  $-7\%$  [28].

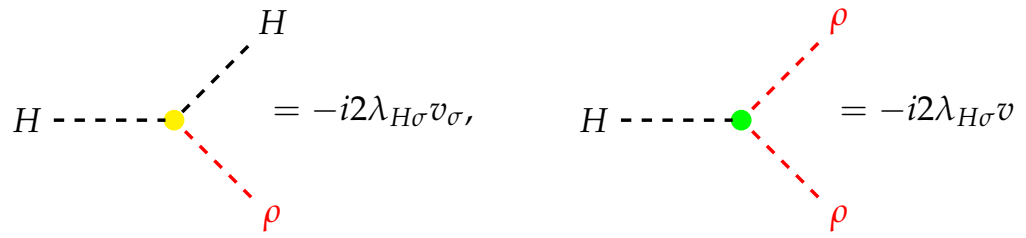


**Figure 1.** Vertex factors on trilinear vertices involving both SM Higgs boson and a real singlet  $\rho$ . They can be derived from Eq. (2). We denote  $\rho$  and its propagator by red colour.

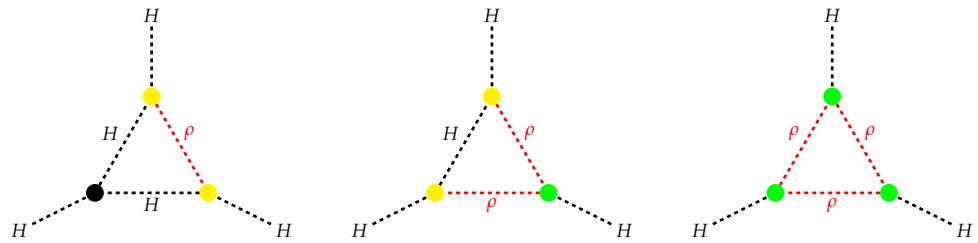


**Figure 2.** One-loop corrections to SM triple Higgs coupling induced by the existence of an extra scalar singlet.

**Light neutrino masses:** The neutrino sector of SMASH is able to generate correct neutrino masses and observe the baryon asymmetry of the universe with suitable benchmarks. The relevant Yukawa terms for neutrinos in the model are

$$\mathcal{L}_\nu^Y = -\frac{1}{2} Y_n^{ij} \sigma N_i N_j - Y_\nu^{ij} L_i \varepsilon H N_j. \quad (17)$$

We take a simplified approach: Dirac and Majorana Yukawa matrices ( $Y_\nu$  and  $Y_n$ , respectively) are assumed to be diagonal.

$$Y_\nu = \begin{pmatrix} y_1 & 0 & 0 \\ 0 & y_2 & 0 \\ 0 & 0 & y_3 \end{pmatrix}, \quad Y_n = \begin{pmatrix} Y_1 & 0 & 0 \\ 0 & Y_2 & 0 \\ 0 & 0 & Y_3 \end{pmatrix}. \quad (18)$$

To generate baryonic asymmetry in the universe, SMASH utilizes the thermal leptogenesis scenario [40], which generates lepton asymmetry in the early universe and leads to baryon asymmetry. In the scenario, heavy neutrinos require a sufficient mass hierarchy [41,42] and one or more Yukawa couplings must have complex CP phase factors. We assume the CP phases are  $\mathcal{O}(1)$  radians to near-maximize the CP asymmetry [43–45]

$$\varepsilon_{\text{CP}} = \frac{\Gamma(N_1 \rightarrow H + \ell_L) - \Gamma(N_1 \rightarrow H^\dagger + \ell_L^\dagger)}{\Gamma(N_1 \rightarrow H + \ell_L) + \Gamma(N_1 \rightarrow H^\dagger + \ell_L^\dagger)} \lesssim \frac{3M_1 m_3}{16\pi v^2}. \quad (19)$$

The largest value is obtained if the CP violation is maximal. A large asymmetry is needed to produce matter-antimatter asymmetry in the universe. Following [37], we set the heavy neutrino mass hierarchy at  $M_3 = M_2 = 3M_1$ , corresponding to  $Y_3 = Y_2 = 3Y_1$ . These choices give the full  $6 \times 6$  neutrino mass matrix

$$M_\nu = \begin{pmatrix} \mathbf{0}_{3 \times 3} & m_D \\ m_D^T & M_M \end{pmatrix}, \quad (20)$$

Benchmarks	BP1	BP2	BP3
$Y_{11}^\nu$	$1.118 \times 10^{-7}$	$1.312 \times 10^{-5}$	$9.610 \times 10^{-6}$
$Y_{22}^\nu$	$7.754 \times 10^{-4}$	$5.347 \times 10^{-4}$	$1.893 \times 10^{-3}$
$Y_{33}^\nu$	$1.878 \times 10^{-3}$	$1.309 \times 10^{-3}$	$4.582 \times 10^{-3}$
$Y_{11}^N$	$9.947 \times 10^{-3}$	$9.614 \times 10^{-3}$	$8.423 \times 10^{-3}$
$Y_Q$	$10^{-3}$	$10^{-3}$	$10^{-3}$
$v_\sigma$ (GeV)	$10^{11}$	$5 \times 10^{10}$	$7 \times 10^{11}$
$\lambda_\sigma$	$7.2 \times 10^{-9}$	$4.48 \times 10^{-7}$	$2.48 \times 10^{-7}$
$\lambda_{H\sigma}$	$-3 \times 10^{-5}$	$-2.25 \times 10^{-4}$	$-1.67 \times 10^{-4}$

**Table 1.** Used benchmark points (BP) in our analysis. Note that we assume specific texture to right-handed neutrino Yukawa matrix  $Y^n$ .

Parameter	$m_t^{\overline{\text{MS}}}(m_t)$	$m_b$	$m_H$	$m_\tau$	$v$	$g_1$	$g_2$	$g_3$	$\lambda_H$
Value	164.0	4.18	125.18	1.777	246.22	0.357	0.652	1.221	0.126

**Table 2.** Used SM inputs in our analysis, at  $\mu = m_Z = 91.18$  GeV, with the exception of top mass, which is evaluated at  $\mu = m_t$ . The masses and vacuum expectation values are in GeV units.

which is in block form, and contains two free parameters:  $v_\sigma$  and  $Y_1$ . Here  $m_D = Y_\nu v / \sqrt{2}$  is the Dirac mass term and  $M_M = Y_n v_\sigma / \sqrt{2}$  is the Majorana mass term. Light neutrino masses are then generated via well-known Type I seesaw mechanism [4–14], by block diagonalizing the full neutrino mass matrix  $M_\nu$ .

It is possible to obtain light neutrino masses consistent with experimental constraints from atmospheric and solar mass splittings  $\Delta m_{32}^2$  and  $\Delta m_{21}^2$  and cosmological constraint  $m_1 + m_2 + m_3 < 0.12$  eV [46–49] (corresponding to  $m_1 \lesssim 0.03$  (0.055) eV with normal (inverse) neutrino mass ordering), assuming the standard  $\Lambda$ CDM cosmological model.

The light neutrino mass matrix is

$$m_\nu = -\frac{v^2}{\sqrt{2}v_\sigma} Y_\nu Y_n^{-1} Y_\nu^T \quad (21)$$

We assume normal mass ordering:  $m_1 < m_2 < m_3$ . We do not know the absolute masses, but the mass squared differences have been measured by various neutrino oscillation experiments [50]. Nevertheless, their values provide two constraints, leaving three free parameters. However, the heavy neutrino Yukawa couplings  $Y_i$  must be no larger than  $\mathcal{O}(10^{-3})$  to avoid vacuum instability [38].

In addition, an order-of-magnitude estimate of generated matter-antimatter asymmetry (baryon-to-photon ratio) is directly proportional to the CP asymmetry:

$$\eta \equiv \frac{n_B}{n_\gamma} = \mathcal{O}(10^{-2}) \epsilon_{\text{CP}} \kappa, \quad (22)$$

where  $\kappa \sim 0.01 - 0.1$  is an efficiency factor. A more precise value of  $\kappa$  can be determined by solving the Boltzmann equations, which is outside the scope of this study. We will provide suitable benchmark points in the next section.

### 3. Methods

We generate the suitable benchmark points demonstrating different physics aspects of the model in the neutrino sector by fitting in the known neutrino mass squared differences  $\Delta m_{ij}^2$ , assuming normal mass ordering ( $m_1 < m_2 < m_3$ ). This leaves three free neutrino parameters, the values of which we generate by logarithmically distributed random sampling. These are the candidates for benchmark points. We then require that the candidate points are consistent with the bound for the sum of light neutrino masses. The next step is to choose the suitable values of other unknown parameters, using the stability of the vacuum as a requirement.

The authors of [37] have generated the corrections to two-loop  $\beta$  functions of SMASH. We solve numerically the full two-loop 14 coupled renormalization group differential equations with SMASH corrections with respect to Yukawa ( $Y^u, Y^d, Y^e, Y^v, Y^N, Y^Q$ ), gauge ( $g_1, g_2, g_3$ ) and scalar couplings ( $\mu_H^2, \mu_S^2, \lambda_H, \lambda_\sigma, \lambda_{H\sigma}$ ), ignoring the light SM degrees of freedom, from  $M_Z$  to Planck scale. We assume Yukawa matrices are on a diagonal basis, with the exception of  $Y^v$ . We use  $\overline{\text{MS}}$  scheme for the running of the RGE's. Since the top quark  $\overline{\text{MS}}$  mass is different from its pole mass, the difference is taken into account via the relation [51]

$$m_t^{\text{pole}} \approx m_t^{\overline{\text{MS}}} \left( 1 + 0.4244\alpha_3 + 0.8345\alpha_3^2 + 2.375\alpha_3^3 + 8.615\alpha_3^4 \right), \quad (23)$$

where  $\alpha_3 \equiv g_3^2/4\pi \approx 0.1085$  at  $\mu = m_Z$ . We define the Higgs quadratic coupling as  $\mu_H = m_H/\sqrt{2}$  and quartic coupling as  $\lambda_H = m_H^2/2v^2$ .

We use MATLAB R2019's `ode45`-solver. See Table 1 for used SMASH benchmark points, and Table 2 for our SM input. Our scale convention is  $t \equiv \log_{10} \mu / \text{GeV}$ .

In some papers, the running of SM parameters ( $Y^t, Y^b, Y^r, g_1, g_2, g_3, \mu_H^2, \lambda_H$ ) obeys the SM RGE's without corrections from a more effective theory until some intermediate scale  $\Lambda_{\text{BSM}}$  [21], after which the SM parameters gain threshold correction (where it is relevant) and the running of all SM parameters follows the new RGE's from that point onwards. We choose to utilize this approach while acknowledging an alternative approach, where the threshold correction is applied at the beginning ( $\mu = m_Z$ ) [22], and both approaches give the almost same results. As previously stated, SM Higgs quadratic and quartic couplings will gain the threshold correction.

Our aim is to find suitable benchmark points, which

- allow the quartic and Yukawa couplings of the theory to remain positive and perturbative up to Planck scale,
- utilize threshold correction mechanism to  $\lambda_H$  via  $\delta \simeq 0.1$ ,
- produce a significant contribution matter-antimatter asymmetry via leptogenesis (requiring hierarchy between the heavy neutrinos), and
- produce a  $\sim 5\%$  correction to triple Higgs coupling  $\lambda_{HHH}$ .

### 4. Results

**Stability of vacuum:** We have plotted how the running of the SM quartic coupling  $\lambda_H$  changes with each benchmark point in Fig. 3. Note that all the threshold corrections are utilized well before the SM instability scale  $\Lambda_{\text{IS}}$ . One can choose  $v_\sigma > \Lambda_{\text{IS}}$  if  $m_\sigma < \Lambda_{\text{IS}}$  is ensured. This is the case with **BP3**.

We numerically scanned over the parameter space  $m_t^{\text{pole}} \in [164, 182] \text{ GeV}$  and  $m_H \in [110, 140] \text{ GeV}$  to analyze vacuum stability in three different benchmark points **BP1-BP3**. Our result for the chosen benchmarks is in Fig. 4, where the SM best fit is denoted by a red star. Clearly the electroweak vacuum is stable with our benchmark points and it assigned to  $m_t^{\text{pole}} \simeq 173.0 \pm 0.4 \text{ GeV}$  and  $m_H \simeq 125.18 \pm 0.16 \text{ GeV}$  [23]. For every case, we investigated the running of the quartic couplings of the scalar potential. We used the following stability conditions:

$$\lambda_H(\mu) > 0, \quad \lambda_\sigma(\mu) > 0, \quad \lambda_H(\mu)\lambda_\sigma(\mu) > \lambda_{H\sigma}(\mu)^2. \quad (24)$$

If one or more conditions are not met on the scale  $\mu \in [m_Z, M_{Pl}]$ , we denote this point unstable. If any of the quartic couplings rises above  $\sqrt{4\pi}$ , we denote this point non-perturbative.

We have chosen the new scalar parameters in such a way that the threshold correction is large but allowed,  $0.1 < \delta < \lambda_H$ . This changes the behaviour of the running so that after the correction the  $\lambda_H$  *increases* in energy instead of decreasing, the opposite to the coupling's running in a pure SM scenario. A too-large threshold correction will have an undesired effect, lowering the nonperturbativity scale to energies lower than the Planck scale. These effects are visualized in Fig. 5, where for each benchmark point kept  $\lambda_\sigma$  at its designated value in Table 1. Instead, we let the portal coupling  $\lambda_{H\sigma}$  vary between 0 and  $\sqrt{0.6\lambda_\sigma}$ . This demonstrates the small range of viable parameters space.

We have also investigated the significance of  $v_\sigma$  on the bounds of threshold correction  $\delta$ . A choice of  $\delta$  is available as long as  $v_\sigma \lesssim 2 \times 10^{13} \text{ GeV}$ . This can be seen clearly from Fig. 6. Given a fixed  $\delta$ , the result is independent of  $\lambda_{H\sigma}$  and  $\lambda_\sigma$ . The lower and higher bound for  $\delta$  increases as a function of  $v_\sigma$ . Instability bound increases, since the needed vacuum-stabilizing threshold effect increases as one approaches the SM instability scale  $\Lambda_{IS}$ . At  $v_\sigma \gtrsim 2 \times 10^{13} \text{ GeV}$ , the  $m_\sigma > \Lambda_{IS}$ , so the quartic coupling  $\lambda_H$  will turn negative before threshold correction is utilized. On the other hand, the nonperturbativity scale increases, since as the cutoff point  $m_\sigma$  increases, the quartic coupling  $\lambda_H$  decreases and correspondingly the largest possible threshold correction increases.

Our next scan was over the new quartic couplings,  $\log_{10}(-\lambda_{H\sigma}) \in [-7, 0]$  and  $\log_{10}\lambda_\sigma \in [-10, 0]$ . The scalar potential is stable and the couplings remain perturbative at only a narrow band, where  $\delta \sim 0.01 - 0.1$ , see Fig. 7. If one considers small  $\delta$ , the SM Higgs quartic coupling will decrease to near zero at  $\mu = M_{Pl}$ . This corresponds to a region near the left side of the stability band. In contrast, we chose our benchmarks with large  $\delta$ , placing it near the right side of the stability band, corresponding to large value of  $\lambda_H$  at  $\mu = M_{Pl}$ . This was a deliberate choice to maximize the correction to  $\lambda_{HHH}$ .

In addition, we have scanned the Dirac neutrino and new quark-like particle Yukawa couplings ( $Y_{11}^\nu$  and  $Y_Q$ , respectively) over  $Y_{11}^\nu \in [0, 2]$  and  $Y_Q \in [0, 0.04]$ , keeping  $Y_{22}^\nu$  and  $Y_{33}^\nu$  small, real<sup>1</sup> and positive but non-zero. See Fig. 8 for details corresponding to each benchmark point. There we have pointed to the area producing a stable vacuum. The Dirac neutrino Yukawa couplings may have a maximum value of  $\mathcal{O}(1)$ , but a more stringent constraint is found for  $Y_Q$ . It should be noted that even though, from the vacuum instability point of view,  $Y_Q^{\max} < Y_{11}^{\nu \max}$ , this does not imply  $Y_Q < Y_{11}^\nu$ , since both are in principle free parameters. See Table 3 for computed values for neutrino masses corresponding to each benchmark.

**Correction to SM triple Higgs coupling:** The real singlet scalar  $\rho$  mixes with the SM Higgs, providing a one-loop correction to SM triple Higgs coupling  $\lambda_{HHH}$ . We scanned the parameter space with  $\log_{10}(-\lambda_{H\sigma}) \in [-7, 0]$  and  $\log_{10}\lambda_\sigma \in [-10, 0]$ . At each point, we calculated the correction to  $\lambda_{HHH}$ . See Fig. 9 for details. We identified a section of parameter space excluded by triple Higgs coupling searches from LHC run 2 and determined the area sensitive to future experiments, namely HL-LHC and FCC-hh. We assume HL-LHC uses 14 TeV center-of-mass energy and integrated luminosity  $\mathcal{L} = 3 \text{ ab}^{-1}$ , for FCC-hh we assume center-of-mass energy 100 TeV and integrated luminosity  $\mathcal{L} = 3 \text{ ab}^{-1}$ . The relative correction in Table 4 is calculated with respect to the SM tree-level prediction. We have chosen our benchmark points in a way that their correction to triple Higgs coupling will be borderline observable at FCC-hh, [52] that is, the correction will be  $\sim 5\%$ . So,  $\eta$  in BP3 for a factor of 10 larger is necessary for stable vacuum and FCC-hh better detection shown in Fig.

<sup>1</sup> We acknowledge that neutrino Yukawa coupling matrix  $Y^\nu$  should be complex in order to allow leptogenesis scenario to work. The vacuum stability analysis, however, is unaffected by this, and we can safely ignore the imaginary parts of the Yukawa couplings in this part of the analysis.

Benchmarks	BP1	BP2	BP3	Experimental values
$m_1$ (meV)	$5.39 \times 10^{-7}$	0.015	$6.71 \times 10^{-4}$	$\lesssim 55$
$m_2$ (meV)	8.64	8.50	8.68	
$m_3$ (meV)	50.67	50.93	50.88	$\lesssim 60$
$m_1 + m_2 + m_3$ (meV)	59.30	59.45	59.57	$< 120$
$\Delta m_{21}^2$ ( $10^{-5}$ eV $^2$ )	7.46	7.22	7.54	6.79 – 8.0
$ \Delta m_{32}^2 $ ( $10^{-3}$ eV $^2$ )	2.57	2.59	2.59	2.412 – 2.625
$M_1$ (GeV)	$7.03 \times 10^8$	$3.40 \times 10^8$	$4.17 \times 10^9$	Unknown
$M_2, M_3$ (GeV)	$2.11 \times 10^9$	$1.02 \times 10^9$	$1.25 \times 10^{10}$	

**Table 3.** The computed values of neutrino masses, sum of light neutrino masses and light neutrino mass squared differences. These neutrino masses are within experimental limits [46–49].

Benchmarks	BP1	BP2	BP3	Experimental values
$\delta(\mu = m_\sigma)$	0.125	0.113	0.113	None
$m_A$ (eV)	$5.7 \times 10^{-5}$	$1.1 \times 10^{-4}$	$8.1 \times 10^{-6}$	Model-dependent
$m_\rho$ (GeV)	$8.49 \times 10^6$	$3.34 \times 10^7$	$3.49 \times 10^8$	
$\eta$	$\sim 10^{-11}$	$\sim 10^{-11}$	$\sim 10^{-10}$	$(6.0 \pm 0.2) \times 10^{-10}$
$\lambda_H(M_{Pl})$	0.222	0.166	0.149	None
$\lambda_\sigma(M_{Pl})$	$5.44 \times 10^{-9}$	$4.5 \times 10^{-7}$	$2.47 \times 10^{-7}$	
$\Delta\lambda_{HHH}$	–5 %	–5 %	–6 %	$< 1400\%$

**Table 4.** The computed values of threshold correction  $\delta$ , BSM scalar masses  $m_A$  and  $m_\rho$ , baryon-to-photon ratio  $\eta$ , quartic self-couplings at  $M_{Pl}$ , correction to triple Higgs coupling  $\Delta\lambda_{HHH}$  compared to the SM prediction.

9. Future FCC-hh accelerator, which is sensitive to  $\sim 5\%$  deviation of the Standard Model prediction. This is demonstrated by the benchmark points we have chosen. Although the model's stable region allows even smaller deviations, part of the region is still accessible by FCC-hh.

This has implications for a general class of BSM theories, which utilize complex singlet scalar and other new non-scalar fields. If the corrections from non-scalar contributions to SM triple Higgs and quartic couplings are tiny, any large correction to  $\lambda_{HHH}$  (such as, a discrepancy from a SM value measured by HL-LHC) would rule out such a class of theories, including SMASH. It will be up to the HL-LHC experiment to determine whether this is the case.

## 5. Conclusions

We have investigated suitable benchmark scenarios for the simplest SMASH model regarding the scalars and neutrinos, constraining the new Yukawa couplings and scalar couplings via the vacuum stability and theory perturbativity requirements. The model can easily account for the neutrino sector, predicting the correct light neutrino mass spectrum while evading the experimental bounds for heavy sterile right-handed Majorana neutrinos.

In [37], the authors of the SMASH model performed a one-loop RGE analysis of the model and presented the two-loop RGE's. We have extended the analysis to two-loop to gain the increased precision needed for the combined achievement of a stabilized electroweak vacuum and a large enough triple Higgs coupling correction to be sensitive at FCC-hh. To the best of the authors' knowledge, this is the first report on the connection between threshold correction to  $\lambda_H$  and one-loop correction to  $\lambda_{HHH}$ .

We found an interesting interplay between the triple Higgs coupling correction and the SM Higgs quartic coupling correction. Successful vacuum stabilization mechanism (threshold mechanism) in SMASH is consistent with small triple Higgs coupling corrections, requiring it to be at most  $\sim 5\%$ . Since the threshold correction  $\delta$  is proportional to  $\Delta\lambda_{HHH}$ , a large correction to it inevitably leads to large threshold correction. Detecting a  $\lambda_{HHH}$  correction larger than  $\sim 35\%$  is within the sensitivity of future high-luminosity upgrade of the LHC [24]. If detected, it would, therefore, rule out the simplest scalar sector of the model completely. This would force the model to develop nonminimal alternatives, such as an additional scalar doublet or triplet instead of a singlet. These alternatives have been considered by the authors of the SMASH model in their recent updated study [39].

## Acknowledgments

CRD is thankful to Prof. D.I. Kazakov (Director, BLTP, JINR) for support.

## References

1. Aad, G.; et al. Observation of a new particle in the search for the Standard Model Higgs boson with the ATLAS detector at the LHC. *Phys. Lett.* **2012**, *B716*, 1–29, [[arXiv:hep-ex/1207.7214](https://arxiv.org/abs/1207.7214)]. doi:10.1016/j.physletb.2012.08.020.
2. Chatrchyan, S.; et al. Observation of a New Boson at a Mass of 125 GeV with the CMS Experiment at the LHC. *Phys. Lett.* **2012**, *B716*, 30–61, [[arXiv:hep-ex/1207.7235](https://arxiv.org/abs/1207.7235)]. doi:10.1016/j.physletb.2012.08.021.
3. Alekhin, S.; Djouadi, A.; Moch, S. The top quark and Higgs boson masses and the stability of the electroweak vacuum. *Physics Letters B* **2012**, *716*, 214–219. doi:<https://doi.org/10.1016/j.physletb.2012.08.024>.
4. Fritzsch, H.; Gell-Mann, M.; Minkowski, P. Vectorlike weak currents and new elementary fermions. *Physics Letters B* **1975**, *59*, 256–260. doi:[https://doi.org/10.1016/0370-2693\(75\)90040-4](https://doi.org/10.1016/0370-2693(75)90040-4).
5. Minkowski, P.  $\mu \rightarrow e\gamma$  at a Rate of One Out of  $10^9$  Muon Decays? *Phys. Lett.* **1977**, *67B*, 421–428. doi:10.1016/0370-2693(77)90435-X.
6. Gell-Mann, M.; Ramond, P.; Slansky, R. Complex Spinors and Unified Theories. *Conf. Proc.* **1979**, *C790927*, 315–321, [[arXiv:hep-th/1306.4669](https://arxiv.org/abs/1306.4669)].
7. Yanagida, T. Horizontal symmetry and masses of neutrinos. *Conf. Proc.* **1979**, *C7902131*, 95–99.
8. Mohapatra, R.N.; Senjanović, G. Neutrino Mass and Spontaneous Parity Nonconservation. *Phys. Rev. Lett.* **1980**, *44*, 912–915. doi:10.1103/PhysRevLett.44.912.
9. Mohapatra, R.N.; Senjanovic, G. Neutrino Masses and Mixings in Gauge Models with Spontaneous Parity Violation. *Phys. Rev.* **1981**, *D23*, 165. doi:10.1103/PhysRevD.23.165.
10. Schechter, J.; Valle, J.W.F. Neutrino Masses in  $SU(2) \times U(1)$  Theories. *Phys. Rev.* **1980**, *D22*, 2227. doi:10.1103/PhysRevD.22.2227.
11. Magg, M.; Wetterich, C. Neutrino Mass Problem and Gauge Hierarchy. *Phys. Lett.* **1980**, *94B*, 61–64. doi:10.1016/0370-2693(80)90825-4.
12. Glashow, S.L. The Future of Elementary Particle Physics. *NATO Sci. Ser. B* **1980**, *61*, 687. doi:10.1007/978-1-4684-7197-7\_15.
13. Lazarides, G.; Shafi, Q. Neutrino Masses in  $SU(5)$ . *Phys. Lett.* **1981**, *99B*, 113–116. doi:10.1016/0370-2693(81)90962-X.
14. Gelmini, G.B.; Roncadelli, M. Left-Handed Neutrino Mass Scale and Spontaneously Broken Lepton Number. *Phys. Lett.* **1981**, *99B*, 411–415. doi:10.1016/0370-2693(81)90559-1.
15. Bambhaniya, G.; Bhupal Dev, P.S.; Goswami, S.; Khan, S.; Rodejohann, W. Naturalness, Vacuum Stability and Leptogenesis in the Minimal Seesaw Model. *Phys. Rev.* **2017**, *D95*, 095016, [[arXiv:hep-ph/1611.03827](https://arxiv.org/abs/1611.03827)]. doi:10.1103/PhysRevD.95.095016.
16. Abbott, L.F.; Sikivie, P. A Cosmological Bound on the Invisible Axion. *Phys. Lett.* **1983**, *120B*, 133–136. doi:10.1016/0370-2693(83)90638-X.
17. Preskill, J.; Wise, M.B.; Wilczek, F. Cosmology of the Invisible Axion. *Phys. Lett.* **1983**, *120B*, 127–132. doi:10.1016/0370-2693(83)90637-8.
18. Dine, M.; Fischler, W. The Not So Harmless Axion. *Phys. Lett.* **1983**, *120B*, 137–141. doi:10.1016/0370-2693(83)90639-1.
19. Bertolini, S.; Di Luzio, L.; Kolešová, H.; Malinský, M. Massive neutrinos and invisible axion minimally connected. *Phys. Rev.* **2015**, *D91*, 055014, [[arXiv:hep-ph/1412.7105](https://arxiv.org/abs/1412.7105)]. doi:10.1103/PhysRevD.91.055014.
20. Salvio, A. A Simple Motivated Completion of the Standard Model below the Planck Scale: Axions and Right-Handed Neutrinos. *Phys. Lett.* **2015**, *B743*, 428–434, [[arXiv:hep-ph/1501.03781](https://arxiv.org/abs/1501.03781)]. doi:10.1016/j.physletb.2015.03.015.

21. Elias-Miró, J.; Espinosa, J.R.; Giudice, G.F.; Lee, H.M.; Strumia, A. Stabilization of the electroweak vacuum by a scalar threshold effect. *Journal of High Energy Physics* **2012**, *2012*, 31. doi:10.1007/JHEP06(2012)031. 290

22. Lebedev, O. On stability of the electroweak vacuum and the Higgs portal. *The European Physical Journal C* **2012**, *72*, 2058. doi:10.1140/epjc/s10052-012-2058-2. 291

23. Workman, R.L.; et al. Review of Particle Physics. *PTEP* **2022**, *2022*, 083C01. doi:10.1093/ptep/ptac097. 292

24. Cepeda, M.; et al. Report from Working Group 2: Higgs Physics at the HL-LHC and HE-LHC. *CERN Yellow Rep. Monogr.* **2019**, *7*, 221–584, [[arXiv:hep-ph/1902.00134](https://arxiv.org/abs/hep-ph/1902.00134)]. doi:10.23731/CYRM-2019-007.221. 293

25. Arkani-Hamed, N.; Han, T.; Mangano, M.; Wang, L.T. Physics opportunities of a 100 TeV proton–proton collider. *Phys. Rept.* **2016**, *652*, 1–49, [[arXiv:hep-ph/1511.06495](https://arxiv.org/abs/hep-ph/1511.06495)]. doi:10.1016/j.physrep.2016.07.004. 294

26. Baglio, J.; Djouadi, A.; Quevillon, J. Prospects for Higgs physics at energies up to 100 TeV. *Rept. Prog. Phys.* **2016**, *79*, 116201, [[arXiv:hep-ph/1511.07853](https://arxiv.org/abs/hep-ph/1511.07853)]. doi:10.1088/0034-4885/79/11/116201. 295

27. Contino, R.; et al. Physics at a 100 TeV pp collider: Higgs and EW symmetry breaking studies. *CERN Yellow Rep.* **2017**, pp. 255–440, [[arXiv:hep-ph/1606.09408](https://arxiv.org/abs/hep-ph/1606.09408)]. doi:10.23731/CYRM-2017-003.255. 296

28. Baglio, J.; Weiland, C. Heavy neutrino impact on the triple Higgs coupling. *Phys. Rev.* **2016**, *D94*, 013002, [[arXiv:hep-ph/1603.00879](https://arxiv.org/abs/hep-ph/1603.00879)]. doi:10.1103/PhysRevD.94.013002. 297

29. Baglio, J.; Weiland, C. The triple Higgs coupling: A new probe of low-scale seesaw models. *JHEP* **2017**, *04*, 038, [[arXiv:hep-ph/1612.06403](https://arxiv.org/abs/hep-ph/1612.06403)]. doi:10.1007/JHEP04(2017)038. 298

30. Arhrib, A.; Benbrik, R.; Chiang, C.W. Probing triple Higgs couplings of the Two Higgs Doublet Model at Linear Collider. *Phys. Rev.* **2008**, *D77*, 115013, [[arXiv:hep-ph/0802.0319](https://arxiv.org/abs/hep-ph/0802.0319)]. doi:10.1103/PhysRevD.77.115013. 299

31. Dubinin, M.N.; Semenov, A.V. Triple and quartic interactions of Higgs bosons in the general two Higgs doublet model **1998**, [[arXiv:hep-ph/hep-ph/9812246](https://arxiv.org/abs/hep-ph/hep-ph/9812246)]. 300

32. Dubinin, M.N.; Semenov, A.V. Triple and quartic interactions of Higgs bosons in the two Higgs doublet model with CP violation. *Eur. Phys. J.* **2003**, *C28*, 223–236, [[arXiv:hep-ph/hep-ph/0206205](https://arxiv.org/abs/hep-ph/hep-ph/0206205)]. doi:10.1140/epjc/s2003-01141-5. 301

33. Kanemura, S.; Kikuchi, M.; Yagyu, K. Radiative corrections to the Higgs boson couplings in the model with an additional real singlet scalar field. *Nucl. Phys.* **2016**, *B907*, 286–322, [[arXiv:hep-ph/1511.06211](https://arxiv.org/abs/hep-ph/1511.06211)]. doi:10.1016/j.nuclphysb.2016.04.005. 302

34. Kanemura, S.; Kikuchi, M.; Yagyu, K. One-loop corrections to the Higgs self-couplings in the singlet extension. *Nucl. Phys.* **2017**, *B917*, 154–177, [[arXiv:hep-ph/1608.01582](https://arxiv.org/abs/hep-ph/1608.01582)]. doi:10.1016/j.nuclphysb.2017.02.004. 303

35. He, S.P.; Zhu, S.H. One-Loop Radiative Correction to the Triple Higgs Coupling in the Higgs Singlet Model. *Phys. Lett.* **2017**, *B764*, 31–37, [[arXiv:hep-ph/1607.04497](https://arxiv.org/abs/hep-ph/1607.04497)]. doi:10.1016/j.physletb.2016.11.007. 304

36. Aoki, M.; Kanemura, S.; Kikuchi, M.; Yagyu, K. Radiative corrections to the Higgs boson couplings in the triplet model. *Phys. Rev.* **2013**, *D87*, 015012, [[arXiv:hep-ph/1211.6029](https://arxiv.org/abs/hep-ph/1211.6029)]. doi:10.1103/PhysRevD.87.015012. 305

37. Ballesteros, G.; Redondo, J.; Ringwald, A.; Tamarit, C. Standard Model—axion—seesaw—Higgs portal inflation. Five problems of particle physics and cosmology solved in one stroke. *Journal of Cosmology and Astroparticle Physics* **2017**, *2017*, 001. 306

38. Ballesteros, G.; Redondo, J.; Ringwald, A.; Tamarit, C. Unifying Inflation with the Axion, Dark Matter, Baryogenesis, and the Seesaw Mechanism. *Phys. Rev. Lett.* **2017**, *118*, 071802. doi:10.1103/PhysRevLett.118.071802. 307

39. Ballesteros, G.; Redondo, J.; Ringwald, A.; Tamarit, C. Several Problems in Particle Physics and Cosmology Solved in One SMASH. *Front. Astron. Space Sci.* **2019**, *6*, 55, [[arXiv:hep-ph/1904.05594](https://arxiv.org/abs/hep-ph/1904.05594)]. doi:10.3389/fspas.2019.00055. 308

40. Fukugita, M.; Yanagida, T. Baryogenesis without grand unification. *Physics Letters B* **1986**, *174*, 45–47. doi:[https://doi.org/10.1016/0370-2693\(86\)91126-3](https://doi.org/10.1016/0370-2693(86)91126-3). 309

41. Buchmuller, W.; Di Bari, P.; Plumacher, M. Cosmic microwave background, matter - antimatter asymmetry and neutrino masses. *Nucl. Phys.* **2002**, *B643*, 367–390, [[arXiv:hep-ph/hep-ph/0205349](https://arxiv.org/abs/hep-ph/hep-ph/0205349)]. [Erratum: Nucl. Phys.B793,362(2008)], doi:10.1016/S0550-3213(02)00737-X, 10.1016/j.nuclphysb.2007.11.030. 310

42. Davidson, S.; Ibarra, A. A Lower bound on the right-handed neutrino mass from leptogenesis. *Phys. Lett.* **2002**, *B535*, 25–32, [[arXiv:hep-ph/hep-ph/0202239](https://arxiv.org/abs/hep-ph/hep-ph/0202239)]. doi:10.1016/S0370-2693(02)01735-5. 311

43. Buchmüller, W.; Bari, P.D.; Plümacher, M. Leptogenesis for pedestrians. *Annals of Physics* **2005**, *315*, 305 – 351. doi:<https://doi.org/10.1016/j.aop.2004.02.003>. 312

44. Buchmüller, W. Leptogenesis: Theory and Neutrino Masses. *Nuclear Physics B - Proceedings Supplements* **2013**, 235–236, 329 – 335. The XXV International Conference on Neutrino Physics and Astrophysics, doi:<https://doi.org/10.1016/j.nuclphysbps.2013.04.029>. 313

45. Buchmüller, W. Leptogenesis. *Scholarpedia* **2014**, *9*, 11471. revision #144189, doi:10.4249/scholarpedia.11471. 314

46. Aghanim, N.; et al. Planck 2018 results. VI. Cosmological parameters. *Astron. Astrophys.* **2020**, *641*, A6, [[arXiv:astro-ph.CO/1807.06209](https://arxiv.org/abs/astro-ph.CO/1807.06209)]. [Erratum: *Astron.Astrophys.* 652, C4 (2021)], doi:10.1051/0004-6361/201833910. 315

47. Goobar, A.; Hannestad, S.; Mortsell, E.; Tu, H. A new bound on the neutrino mass from the sdss baryon acoustic peak. *JCAP* **2006**, *06*, 019, [[astro-ph/0602155](https://arxiv.org/abs/astro-ph/0602155)]. doi:10.1088/1475-7516/2006/06/019. 316

48. Di Valentino, E.; Gariazzo, S.; Mena, O. Most constraining cosmological neutrino mass bounds. *Phys. Rev. D* **2021**, *104*, 083504, [[arXiv:astro-ph.CO/2106.15267](https://arxiv.org/abs/astro-ph.CO/2106.15267)]. doi:10.1103/PhysRevD.104.083504. 317

49. Vagnozzi, S.; Giusarma, E.; Mena, O.; Freese, K.; Gerbino, M.; Ho, S.; Lattanzi, M. Unveiling  $\nu$  secrets with cosmological data: neutrino masses and mass hierarchy. *Phys. Rev.* **2017**, *D96*, 123503, [[arXiv:astro-ph.CO/1701.08172](https://arxiv.org/abs/astro-ph.CO/1701.08172)]. doi:10.1103/PhysRevD.96.123503. 318

---

50. Esteban, I.; Gonzalez-Garcia, M.C.; Hernandez-Cabezudo, A.; Maltoni, M.; Schwetz, T. Global analysis of three-flavour neutrino oscillations: synergies and tensions in the determination of  $\theta_{23}$ ,  $\delta_{CP}$ , and the mass ordering. *JHEP* **2019**, *01*, 106, [[arXiv:hep-ph/1811.05487](https://arxiv.org/abs/hep-ph/1811.05487)]. doi:10.1007/JHEP01(2019)106. 347

51. Jegerlehner, F.; Kalmykov, M.Yu.; Kniehl, B.A. On the difference between the pole and the  $\overline{MS}$  masses of the top quark at the electroweak scale. *Phys. Lett.* **2013**, *B722*, 123–129, [[arXiv:hep-ph/1212.4319](https://arxiv.org/abs/hep-ph/1212.4319)]. doi:10.1016/j.physletb.2013.04.012. 348

52. He, H.J.; Ren, J.; Yao, W. Probing new physics of cubic Higgs boson interaction via Higgs pair production at hadron colliders. *Phys. Rev.* **2016**, *D93*, 015003, [[arXiv:hep-ph/1506.03302](https://arxiv.org/abs/hep-ph/1506.03302)]. doi:10.1103/PhysRevD.93.015003. 349

53. 350

54. 351

55. 352

56. 353

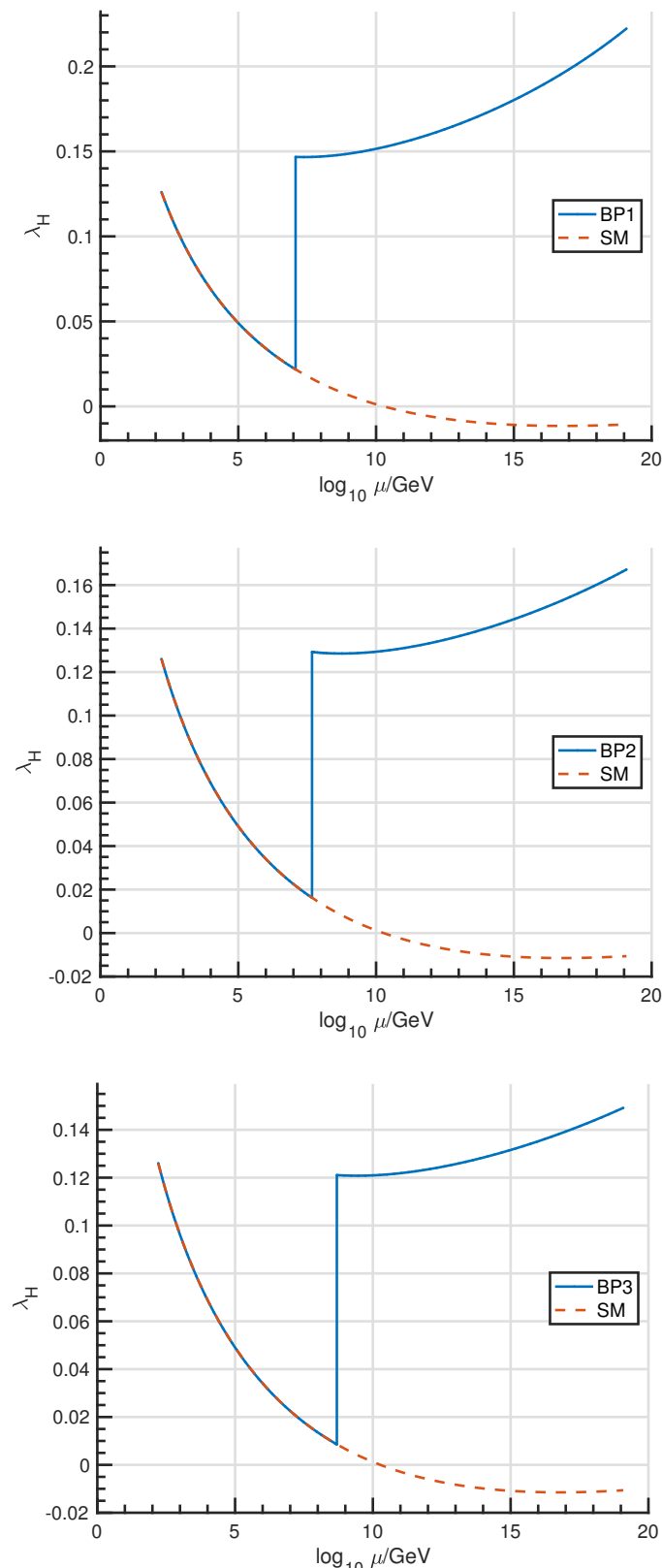


**Figure 3.** Running of SM Higgs quartic coupling in Standard Model (dashed line) and in SMASH with benchmark points **BP1-BP3** (solid line). Threshold correction is utilized at  $m_\rho$ .

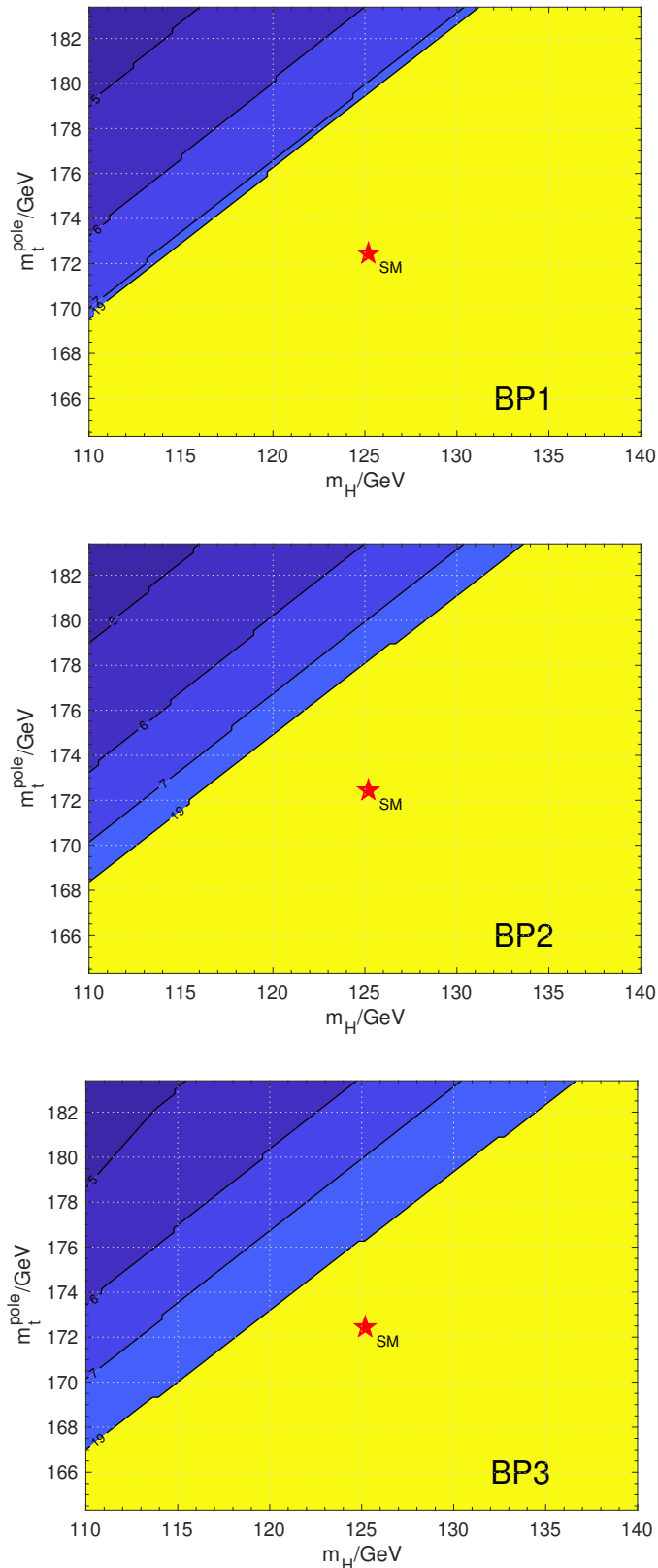


**Figure 4.** Vacuum stability of SMASH in  $(m_H, m_t^{\text{pole}})$  plane with benchmark points **BP1-BP3**. The red star corresponds to the SM best-fit value. The height and width of the star correspond to the present uncertainties. The vacuum is stable in the yellow region. The contour numbers  $n$  correspond to the vacuum instability scale  $10^n \text{ GeV}$ .

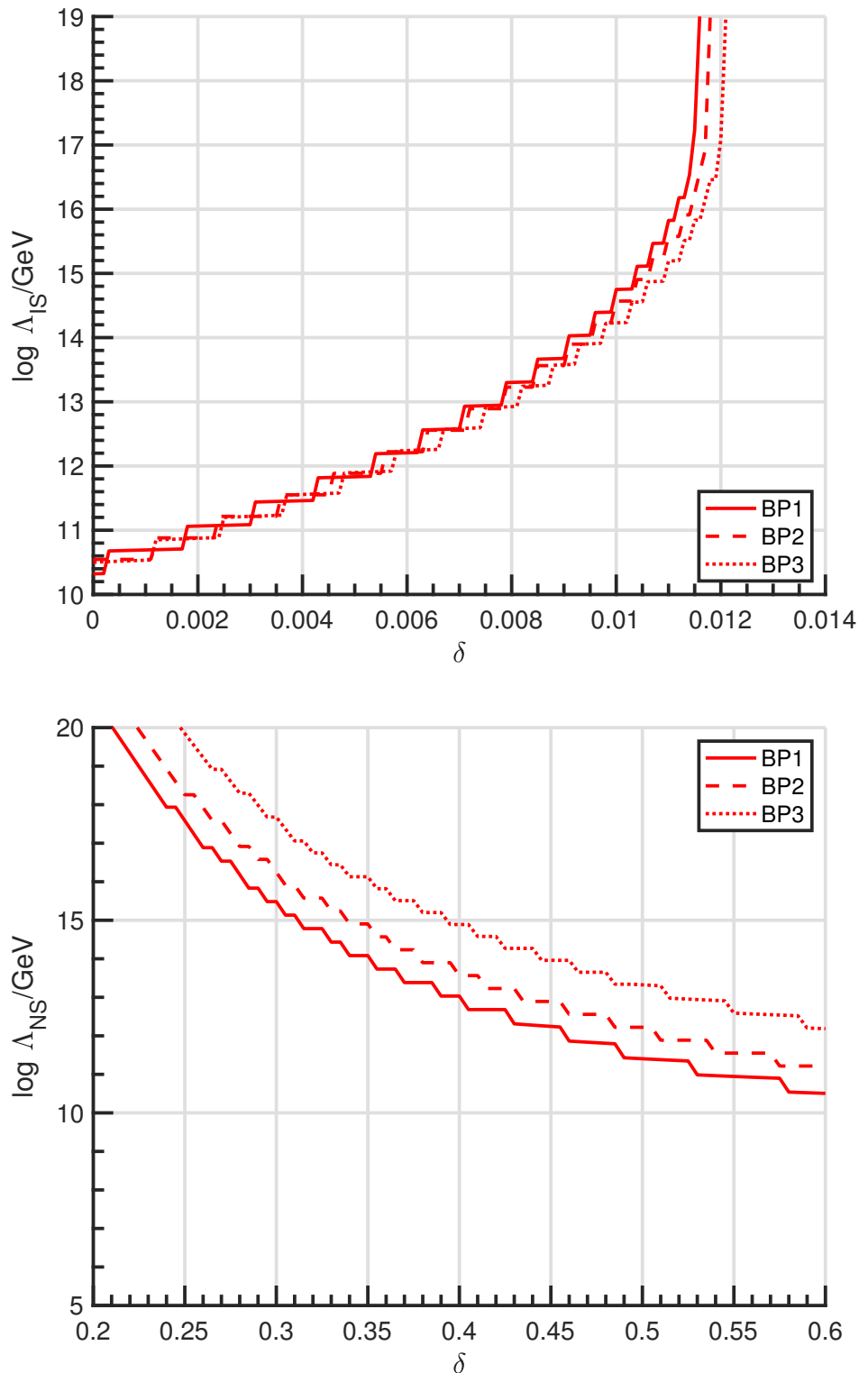


**Figure 5.** The rise of instability scale (above) and the fall of nonperturbativity scale (below) as a function of threshold correction  $\delta$ , for **BP1-BP3**.

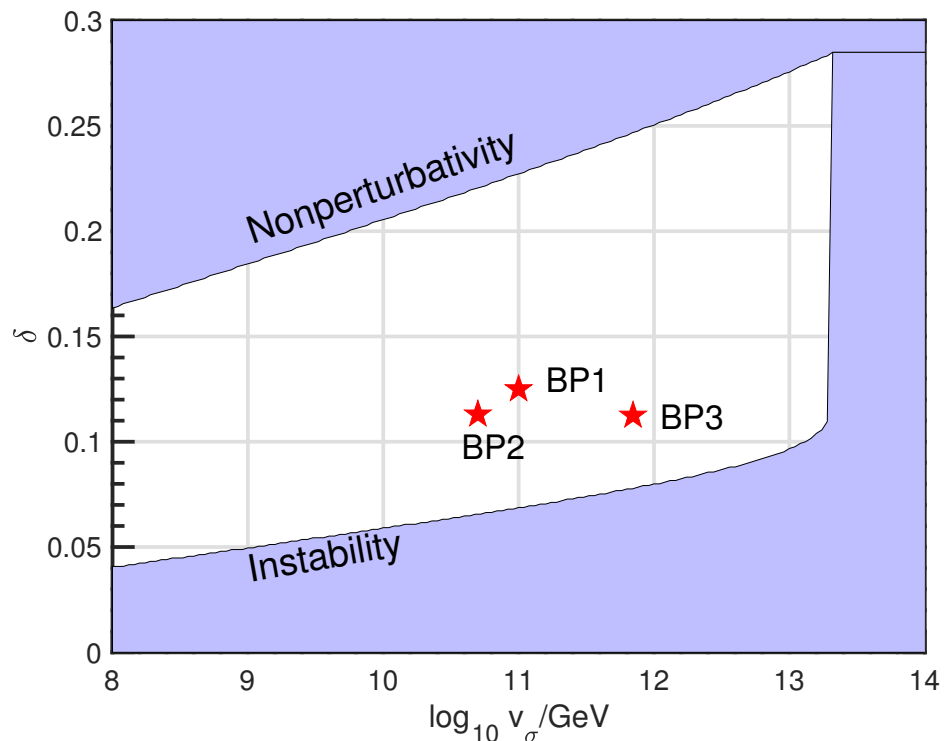


**Figure 6.** The available parameter space is consistent with a stable vacuum in  $(v_\sigma, \delta)$  space.  $\lambda_\sigma$  is fixed, while  $\lambda_{H\sigma}$  is determined by Eq. 12 and  $m_\sigma$  by Eq. 8. We have denoted our benchmark points with a red star.

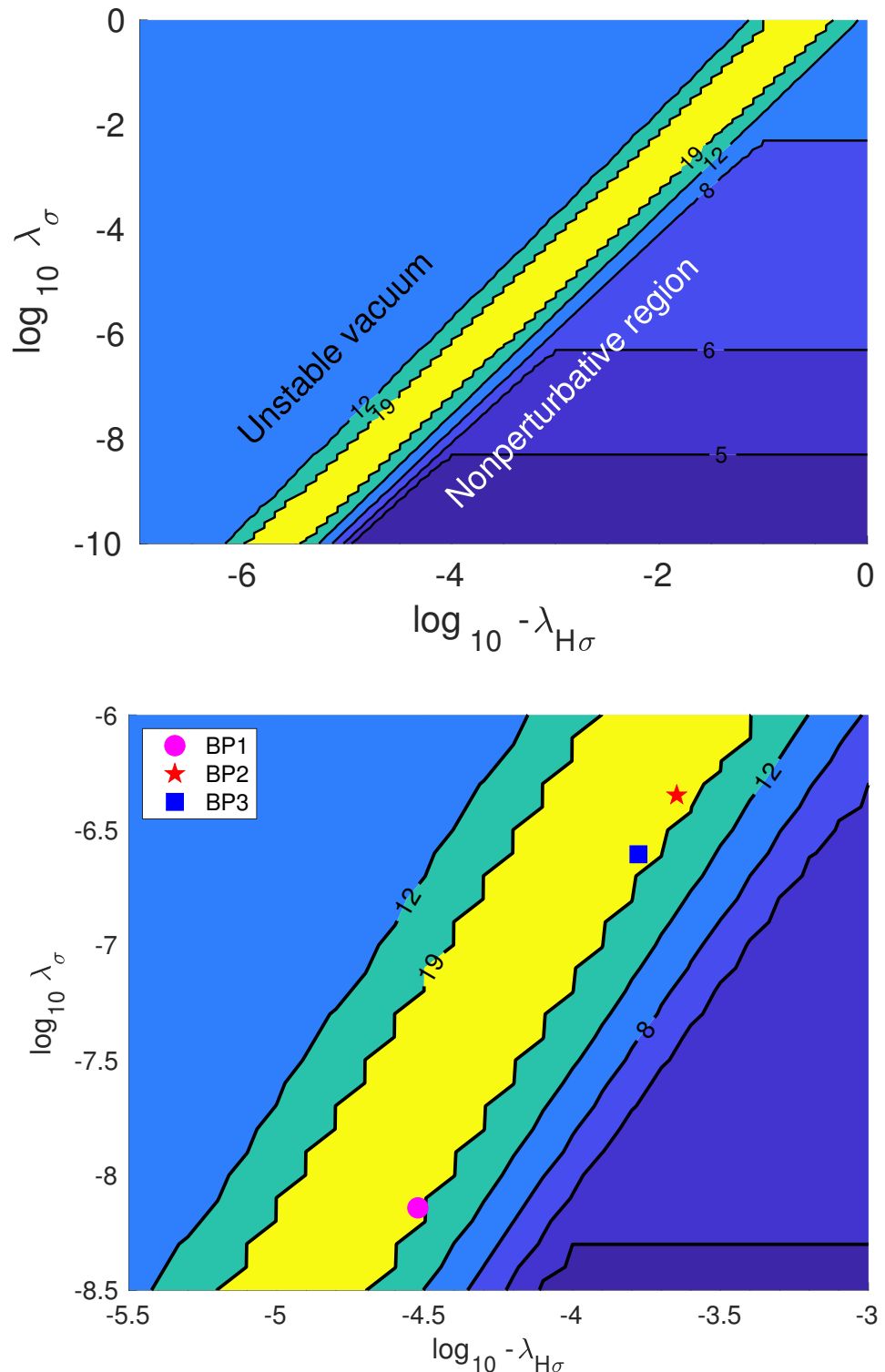


**Figure 7. Above:** Different regions in the logarithmic  $(-\lambda_{H\sigma}, \lambda_\sigma)$  plane. The contour numbers  $n$  above the yellow band correspond to vacuum instability scale  $10^n$  GeV. Below the yellow band the contour numbers  $m$  correspond to nonperturbativity scale  $10^m$  GeV. The colour coding is interpreted as in Fig. 4. For nonperturbative scale calculations, we have used **BP1**. **Below:** Zoomed-in detail of the figure above, showing in addition our chosen benchmarks.

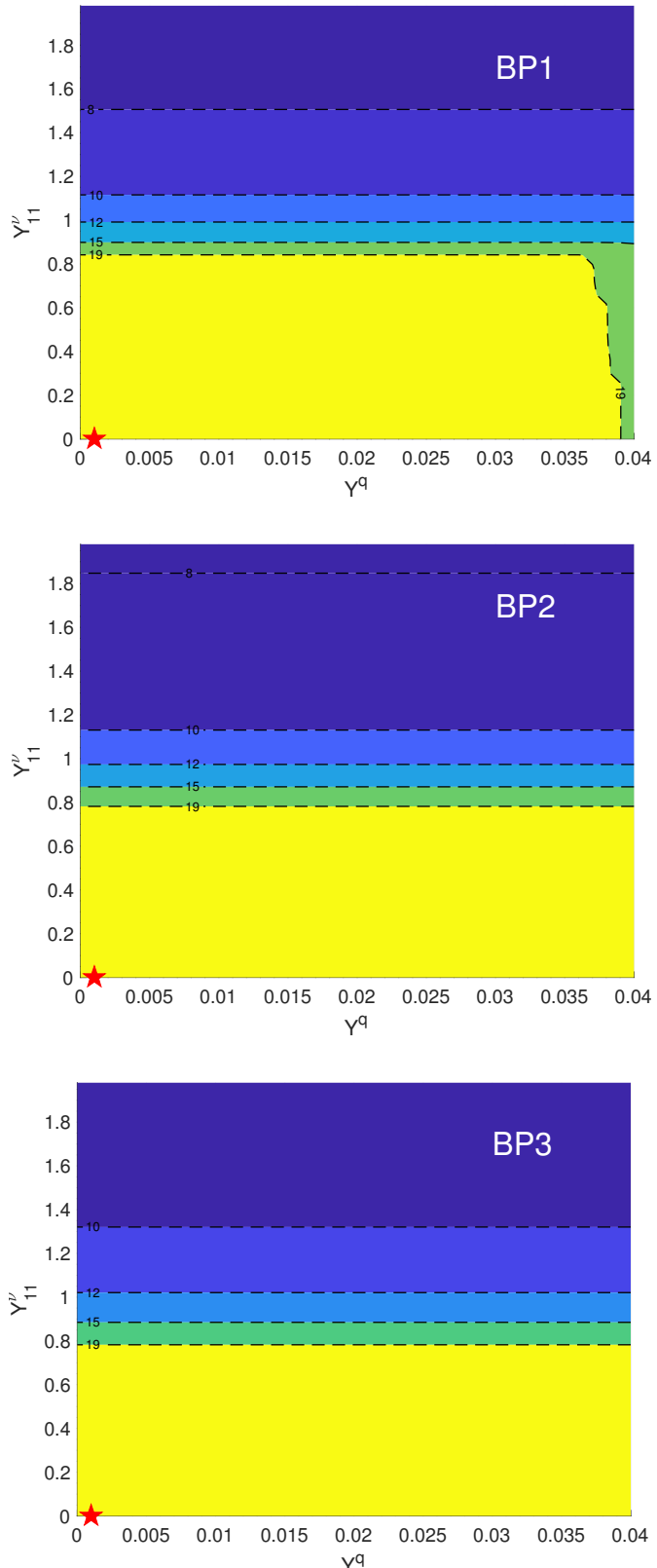


**Figure 8.** Vacuum instability scales in  $(Y^q, Y_{11}^v)$  plane in benchmark points BP1-BP3. The red star corresponds to the chosen benchmark point value. The colour coding and the contour numbers are interpreted as in Fig. 4.

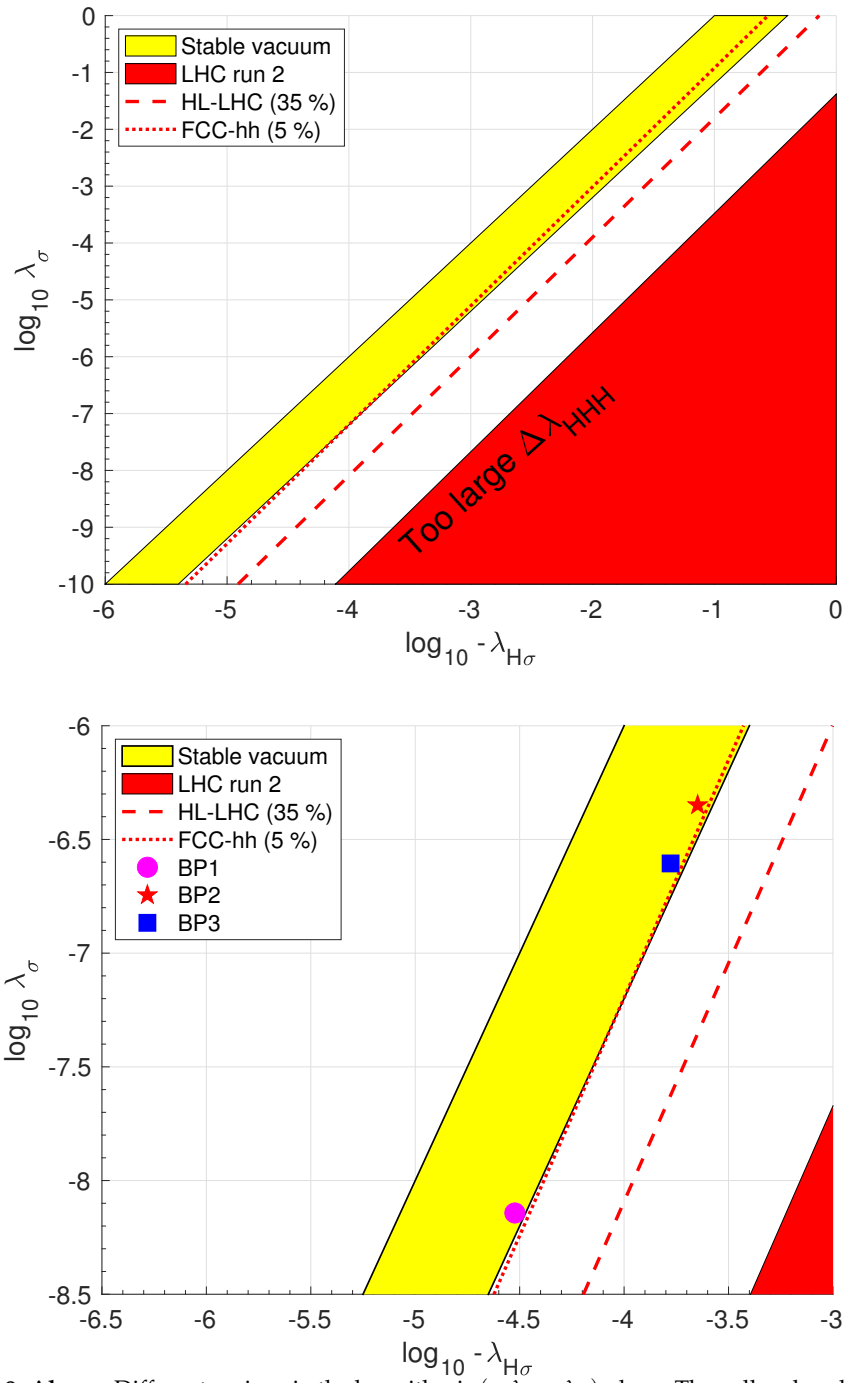


**Figure 9. Above:** Different regions in the logarithmic  $(-\lambda_{H\sigma}, \log_{10} \lambda_\sigma)$  plane. The yellow band corresponds to a stable vacuum configuration. The red area is excluded by the second run of the Large Hadron Collider, since the triple Higgs coupling corrections to SMASH would be too large. The dashed line corresponds to the expected sensitivity of the high-luminosity LHC and the dotted line to the expected sensitivity of the Future Circular Collider in hadronic collision mode. **Below:** Zoomed-in detail of the figure above, showing in addition our chosen benchmarks.